

ments and have shown that the differential averaging technique is practically valid.

REFERENCES

1. G. Birnbaum and J. Franeau, "Measurement of the Dielectric Constant and Loss of Solids and Liquids by a Cavity Perturbation Method," *J. Appl. Phys.* 20, Aug. 1949, pp. 817-818.
2. R. A. Waldron, "Perturbation Theory of Resonant Cavities," *Proc. IEE*, vol. 107C, 1960, pp. 272-274.
3. R. F. Harrington, *Time-Harmonic Electromagnetic Fields*, 1985, Chap. 7.
4. A. Parkash, J. K. Vaid, and A. Mansingh, "Measurement of the Dielectric Parameters at Microwave Frequencies by Cavity Perturbation Technique," *IEEE Trans. Microwave Theory Tech.*, Vol. MTT-27, No. 9, 1979, pp. 791-795.
5. A. Mansingh and A. Parkash, "Microwave Measurement of Conductivity and Permittivity of Semiconductor Sphere by Cavity Perturbation Technique," *IEEE Trans. Microwave Theory Tech.*, Vol. MTT-29, No. 1, 1981, pp. 65-67.
6. S. H. Chao, "Measurements of Microwave Conductivity and Dielectric Constant by the Cavity Perturbation Method and Their Errors," *IEEE Trans. Microwave Theory Tech.*, Vol. MTT-33, No. 6, 1985, pp. 519-526.
7. A. W. Kraszewski and S. O. Nelson, "Observations on Resonant Cavity Perturbation by Dielectric Objects," *IEEE Trans. Microwave Theory Tech.*, Vol. MTT-40, No. 1, 1992, pp. 151-155.
8. K. T. Mathew and U. Raveendranath, "Waveguide Cavity Perturbation Method for Measuring Complex Permittivity of Water," *Microwave Opt. Technol. Lett.*, Vol. 6, No. 2, 1993, pp. 104-106.
9. O. Svelto, *Principles of Lasers*, Plenum Press, Chap. 2.

Received 3-29-96; revised 5-17-96

Microwave and Optical Technology Letters, 13/2, 87-90

© 1996 John Wiley & Sons, Inc.

CCC 0895-2477/96

OPTIMIZATION OF THE RF CIRCUIT FOR WIDE-BANDWIDTH CROSS-LINKED POLYMER ELECTRO-OPTIC MODULATORS

Hung Nguyen,* George E. Ponchak, Richard Kunath, Donna Bohman, and Nick Varlajay

NASA Lewis Research Center
Space Communications Division
Mail Stop 54-8
21000 Brookpark Road
Cleveland, Ohio 44135

KEY TERMS

Optical modulation, losses, optical polymers, tapered waveguides

ABSTRACT

A transmission-line theory approach that includes the complex propagation constant of the microwave electrodes and the impedance match between the electrode and the rf source and load is used to analyze the bandwidth of polyamide optical modulators. The analysis is then applied to an electro-optic modulator that has microstrip transmission lines placed directly over an optical waveguide buried in the polyamide substrate. The modulator is designed with coplanar waveguide (CPW) input and output contacts for rf characterization. The transition between

* Also with Department of Electrical Engineering & Applied Physics, Case Western Reserve University, Cleveland, Ohio

the microstrip electrode and the CPW lines is presented. In addition, the processing techniques that yield polyamide side-wall profiles that are highly suited for transitioning from the CPW and the microstrip are presented. Finally, rf measurements of the complete microwave electrode are presented. © 1996 John Wiley & Sons, Inc.

I. INTRODUCTION

High-speed optical modulators are essential components in wideband or high-data-rate fiber-optic communication systems. Recently, significant progress has been made in the development of these modulators employing nonlinear polymer materials [1-3]. Some of the advantages these materials have for high-speed devices are potentially large electro-optic (EO) coefficients, low dielectric constants, and small dispersion from microwave through optical frequencies [4]. As a direct result of these material properties, modulators with lower operating voltages and larger bandwidths are possible [3, 5].

Many electro-optic modulators have been reported [6], but the bandwidth has been limited by the difference in velocity between the optical and microwave signals traveling through the modulator, the loss of the rf transmission lines, and the impedance mismatch at the rf input and output ports. In traveling-wave modulators, the modulating rf and the optical signals propagate along separate transmission lines that are tightly coupled. Therefore, the coupling efficiency of these modulators is determined by the velocity match between the two propagating waveguides, or the upper frequency response is determined by the difference between the rf and optical phase velocities. Hence, for ultimate efficiency and bandwidth, both velocities should be equal. This is equivalent to saying that the square root of the effective dielectric constant at the microwave frequency and the refractive index of the polymer material at the optical frequency are equal [2]. For microstrip lines on low-dielectric-constant polymers, the predicted effective dielectric constant can be as low as 2.6 which is close to the square of the refractive index of polymer materials, about 1.5-2.0 [7, 8]. Therefore, the velocity match is not a limiting factor in the polymer-based modulators. Instead, the microwave attenuation and the impedance match are the limiting factors in the modulator bandwidth.

Recently, considerable effort has been made to improve the fabrication technology of optical polymer devices [9]. In addition, there have been several papers outlining the design of electro-optic modulators employing CPW electrodes. However, the design optimization of high-speed, polyamide modulators with microstrip electrodes has not been reported. A number of design parameters need to be optimized if practical device performance is to be achieved. Specifically, the microstrip width and height needs to be selected to minimize the microwave loss, the impedance match, and the velocity match simultaneously. Alternatively, the width and height of the microstrip need to be selected to optimize the frequency response of the modulator when fabrication or other constraints are placed upon the design.

In this article we present the design and analysis of a microstrip electrode fabricated on a polyamide surface and coupled to the microwave input and output ports through coplanar waveguide (CPW). This electrode structure was designed to provide a very high modulation bandwidth. Microwave measurements of the rf electrode circuit are presented. In addition, the effective dielectric constant and loss of the microstrip line is presented. Based on the electrode design, the predicted small-signal bandwidth of the modula-

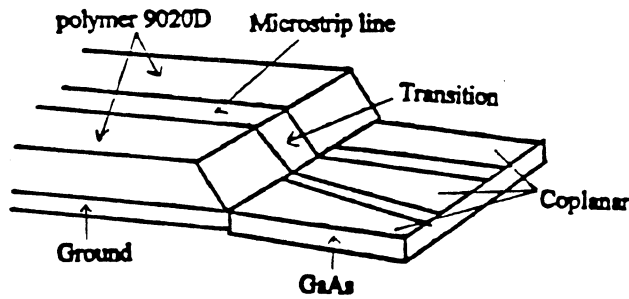


Figure 1 A section of microstrip-coplanar transition on cross-linked polymer

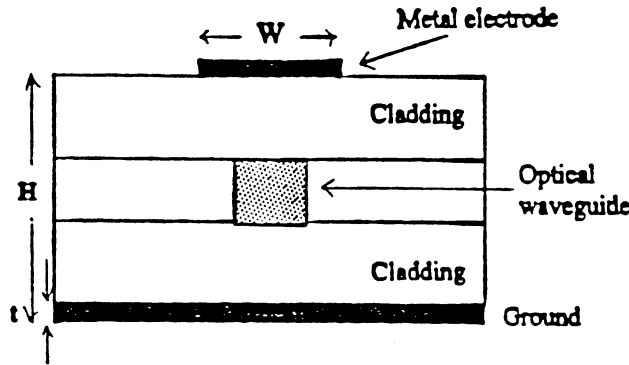


Figure 2 A cross section of the optical waveguide-microstrip line

tor, primarily limited by microwave losses, can exceed more than 40 GHz.

II. DESIGN PROCEDURE

Figure 1 shows the electro-optic modulator that is characterized in this article. It consists of a microstrip line placed directly over the optical waveguide as shown in Figure 2. Therefore, the field interaction should be large compared to modulators relying on slot-line or CPW electrodes, and the switching voltage, $V\pi$, should be lower. Coplanar waveguides are fabricated on the substrate to provide access for microwave probes or coaxial to CPW launchers. An impedance matching taper is incorporated into the CPW. In addition, a transition is required from the CPW on the substrate to the microstrip line on the polyamide layers.

To characterize the electrode structure, the microstrip characteristic impedance Z_0 , the microstrip propagation constant $\gamma = \alpha + j\beta$, the length of the coupling region L , the source voltage V_0 , and the source and load impedances, Z_s and Z_L , are required [10]. Although the parameters assumed a microstrip line, these parameters are general and apply to any electrode structure. Therefore, this part of the design is not limited to the structure defined in Figure 1. A single-frequency collinear electrical signal at any point along the microstrip line can be obtained as [11]

$$V(z, t_0) = V(z) \sin\left(\frac{2\pi f \Delta n}{c} z - 2\pi f t\right), \quad (1)$$

where c is the speed of light, f is the microwave frequency, $V(z)$ is the voltage vector at any point z along the transmission line, and Δn is the difference between the microwave and the optical refractive indices. The function $V(z)$ can be

described as

$$V(z) = V_0 \frac{e^{-\gamma z} + \rho_L e^{-2\gamma L} e^{\gamma z}}{1 - \rho_s \rho_L e^{-2\gamma L}}, \quad (2)$$

where ρ_s and ρ_L are the reflection coefficients at the source and load. Δn is defined as

$$\Delta n = \sqrt{\epsilon_{\text{eff}}} - n \quad (3)$$

where ϵ_{eff} is the effective dielectric constant at the microwave frequency and n is a refractive index at the optical frequency. For devices that operate by accumulated phase shift, such as phase modulators and Mach-Zehnder amplitude modulators, the total phase shift $\Delta\phi$ can be obtained by integrating Eq. (1) over the active length of the structure. This results in

$$\Delta\phi = \delta \int_0^L V(z) \sin\left(\frac{2\pi f \Delta n}{c} z - 2\pi f t\right) dz, \quad (4)$$

where δ the resulting phase shift for polarized light after an interaction length L and can be written as

$$\delta = \frac{\pi n^3 r V_0 \Gamma L}{\lambda H}. \quad (5)$$

Here r is the pertinent electro-optic coefficient, H is the microstrip substrate or the polyamide thickness, and Γ is the electrical-optical overlap parameter. From Eq. (4), the total optical phase shift can be expressed as

$$\Delta\phi = \frac{\delta}{1 - \rho_L \rho_s e^{-2\alpha L}} \times \sqrt{\frac{a^2 + b^2}{e^{2\alpha L}((KL)^2 + (\alpha L)^2)^2}} \sin(\Phi - 2\pi f_m t), \quad (6)$$

where

$$a = L(K \cos(KL) + \alpha \sin(KL) - Ke^{\alpha L}) + LT(e^{2\alpha L} K \cos(KL) - e^{2\alpha L} \alpha \sin(KL) - K), \quad (7)$$

$$b = L(K \sin(KL) - \alpha \cos(KL) + \alpha e^{\alpha L}) + LT(e^{2\alpha L} K \sin(KL) + e^{2\alpha L} \alpha \cos(KL) - \alpha), \quad (8)$$

$$T = \rho_L \rho_s e^{-2\alpha L}, \quad (9)$$

and $K = (2\pi f \Delta n)/c$. Equation (6) is a general result that applies to any electrode structure. The phase delay Φ describing the phase difference between the rf and optical wave is given by

$$\Phi = \tan^{-1} \frac{a}{b}. \quad (10)$$

According to Eq. (6), the frequency-dependent amplitude response of the modulator is directly related to $\Delta\phi$ and is given by

$$R(f) = 20 \log \sqrt{\frac{a^2 + b^2}{e^{2\alpha L} (1 - \rho_s \rho_L e^{-2\alpha L})^2 ((KL)^2 + (\alpha L)^2)^2}} + P_{\text{rf}}. \quad (11)$$

In Eq. (11), P_{rf} is the required rf drive power. For a given electrode length, it is found from Eq. (11) that the bandwidth of the modulator is limited by the velocity mismatch between the microwave and optical waveguides, the attenuation of the microwave transmission line, and reflections caused by impedance. Because of the small difference between the optical and microwave refractive index, polyamide-based, electro-optic modulators are not limited by Δn . Thus, it is predominantly the attenuation and the reflections that limit the 3-dB bandwidth of the modulators.

To characterize the specific structure shown in Figure 1, the microstrip and CPW transmission lines must be characterized [12, 13]. To determine the microstrip propagation constant, the equations of Hammersted and Jensen were used to determine the static effective dielectric constant, and the equations of Kirshning and Jansen were used to determine the frequency-dependent effective dielectric constant. The attenuation constant was determined from Bhartia's equations, and the characteristic impedance was determined using Hammersted's equations. A 50- Ω impedance was assumed at the input and output ports. Last, the optical index of refraction was assumed to be 1.61.

With the use of the stated equations, the modulator amplitude response $R(f)$, was calculated for four polyamide thicknesses and a range of microstrip widths W at 50 GHz. These results are shown in Figure 3. For the same parameters, the microstrip attenuation and the reflection coefficients ρ_s and ρ_l are shown in Figure 4. It is seen that $R(f)$ has a minimum for a given W and H that corresponds to the minimum in the reflection coefficients. Therefore, the width and height of the microstrip line can be selected to improve the bandwidth frequency of devices. For example, the amplitude response for a width of 15 μm and a height of 6 μm is -2.2 dB at 50-GHz frequency, whereas a width of 10 μm for the same height has a response of -3 dB. Furthermore, the maximum $R(f)$ is greater for thicker polyamides that yield lower microstrip attenuation. The sensitivity of the responsivity to variations in polyamide thickness for a 15-mm-wide line is shown in Figure 5. Note that there is a 15-GHz improvement in bandwidth created by a 4- μm decrease in the polyamide thickness. The associated microstrip attenuation and return loss for the structure is shown in Figure 6 (a

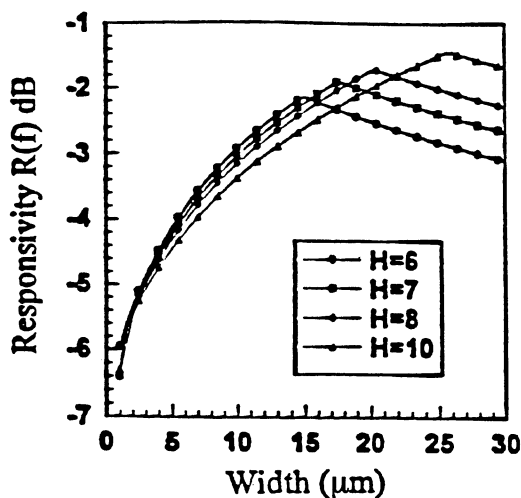


Figure 3 Calculated modulator amplitude response as a function of microstrip width and height

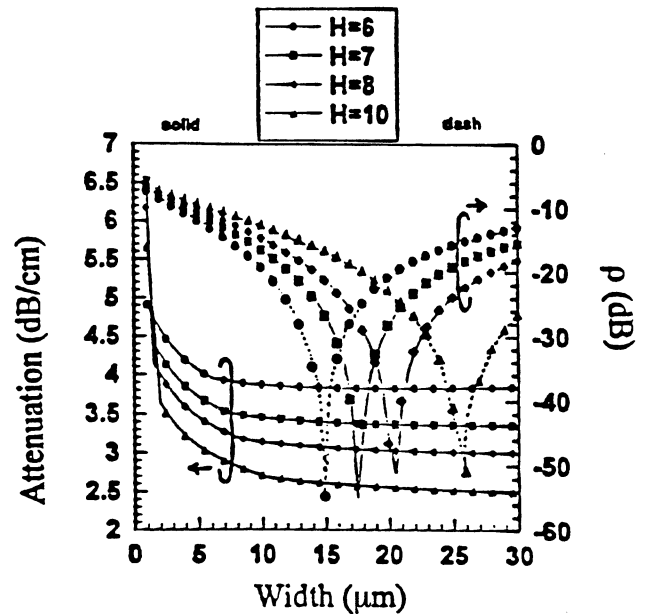


Figure 4 Calculated microstrip attenuation and electrode reflection coefficient as a function of width

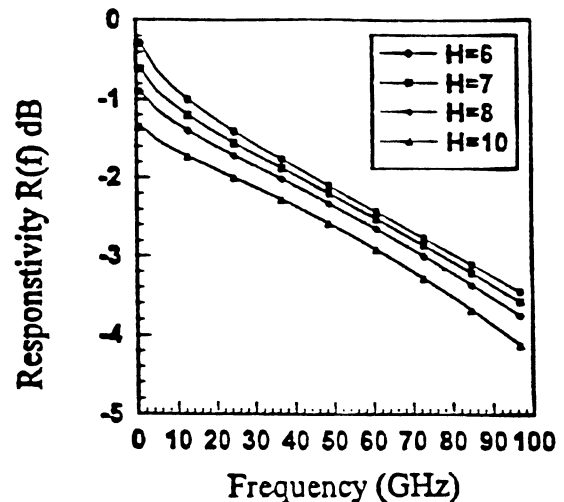


Figure 5 Calculated modulator amplitude response versus frequency for a microstrip width of 15 μm

1.5- μm -thick gold line was assumed). It is seen that although the attenuation varies by 1.5 dB/cm at 50 GHz, the return loss varies by 40 dB for a 4- μm variation in the polyamide thickness. Therefore, it is the sensitivity of the microstrip impedance to substrate variations that is most critical. Whereas the line width is easily controlled by lithography techniques, the polyamide thickness is controlled only by the spin speed and time. Therefore, it is harder to control and can be expected to have a negative impact on the modulator bandwidth.

III. EXPERIMENTS

A microstrip/coplanar waveguide electrode structure with a microstrip length, field-coupling length, of 1.2 cm and a CPW taper length of 0.5 cm was fabricated on 9020D polyamide. First, the CPW and microstrip ground planes, 1.5- μm Au,

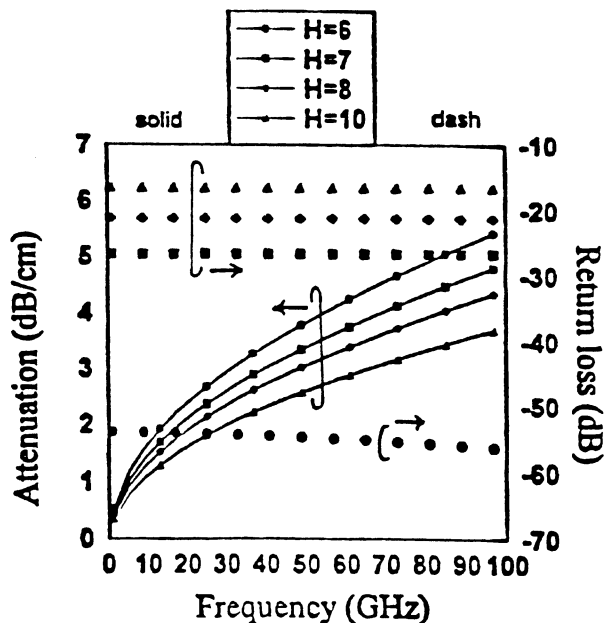


Figure 6 Calculated microstrip attenuation and return loss as a function of frequency for 15- μm -width line

were evaporated onto a standard GaAs wafer. This was followed by spinning on 6 μm of polyamide. Third, a wet etch that was optimized to provide sloped wall profiles was used to remove the polyamide from the CPW lines. Last, the CPW center conductor and microstrip line were evaporated onto the wafer. Standard lift-off processing was used for all of the metallization steps. The Ultradel 9020D polyamide has an ϵ_r of 2.6 and a $\tan \delta$ of 0.002.

All rf characterizations were performed on a HP 8510C network analyzer with GGB Picoprobes. The system was calibrated to the probe tips using an open, short, load calibration. To verify the calculation effective dielectric constant and microstrip attenuation, a TRL calibration using the NIST

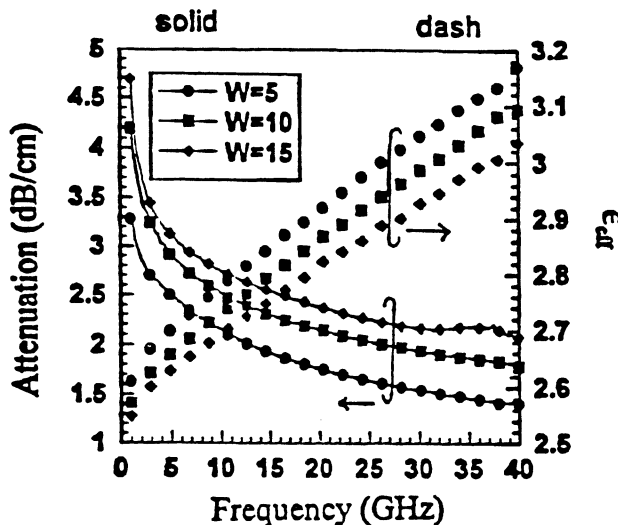


Figure 7 Measured attenuation and effective dielectric constant of microstrip line on 6.5- μm polyamide

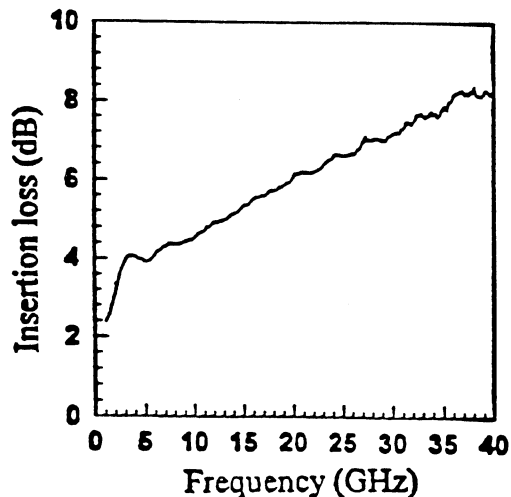


Figure 8 Measured insertion loss as a function of frequency of waveguide electrode

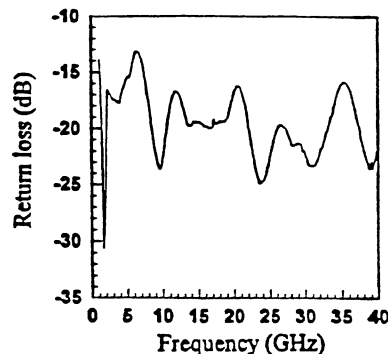


Figure 9 Measured return loss as a function of frequency of waveguide electrode

software MultiCal was used. Figure 7 shows the measured characteristics for a microstrip on a 6.5-mm-thick polyamide. It is first noted that the ϵ_{eff} has a negative slope due to the conductor losses. Furthermore, it is greater than the polyamide ϵ_r of 2.6. Even with these characteristics, Δn is small; the index of refraction of a poled polymer is about 1.61. The measured attenuation is in agreement with the calculated values. Figures 8 and 9 show the measured insertion loss $|S_{21}|$ and return loss as a function of frequency for the entire electrode structure. Approximately half of the electrode insertion loss is due to the microstrip attenuation. The remainder is caused by the length of CPW, the CPW to microstrip transition, and the probe to CPW transition. S_{11} is also measured, and peak reflections of -13 to -23 dB were observed with the use of a cosine-squared taper, indicating good impedance match of the transmission lines to the 50- Ω impedance of the set test. With these measured values, the predicted responsivity of a modulator is plotted versus frequency in Figure 10. A bandwidth of more than 40 GHz is predicted.

IV. CONCLUSION

We have proposed and tested a novel design for the electrode of a high-speed cross-link polymer modulator. An extensive

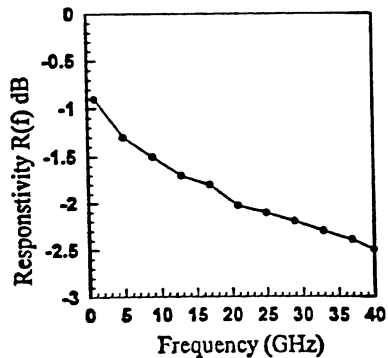


Figure 10 Predicted responsivity $R(f)$ of polymer EO modulator

design analysis of the electrode was discussed, and experimental results were presented to validate the design. It is found that consideration of proper width, height, and impedance matching is critical to improving the 3-dB bandwidth modulation frequency. Furthermore, it was shown that the modulator performance is very sensitive to the polyamide thickness, which is not well controlled in the processing. This type of electrode is applicable to a Mach-Zehnder intensity modulator.

REFERENCES

1. H. Man, K. Chiang, D. Haas, and C. C. Teng, "Polymeric Materials for High Speed Electrooptic Waveguide Modulators," *SPIE*, Vol. 1213, 1990, p. 7.
2. Y. Choi, "Recent Advances in Electro-Optic Devices, Components and System for Microwave and Millimeter-Wave Applications," *Int. J. Infrared Millimeter Waves*, Vol. 16, 1995, pp. 1261.
3. P. R. Ashley and T. A. Tumolillo, "Overview of EO Polymers for Guided Wave Devices," *SPIE Proc.*, Vol. 1583, 1991, p. 316.
4. C. C. Teng, "Traveling Wave Polymeric Optical Intensity Modulator with More than 40 GHz of 3 dB Electrical Bandwidth," *Appl. Phys. Lett.*, Vol. 60, 1992, p. 1538.
5. Rick Lytel, "Applications of Electro-Optic Polymers to Integrated Optics," *SPIE*, Vol. 1216, 1990, p. 30.
6. P. R. Ashley and T. A. Tumolillo, "Overview of EO Polymers for Guided Wave Devices," *SPIE Proc.*, Vol. 1583, 1991, p. 316.
7. W. Yong, Q. Lanfen, and L. Ye, "Computer-Aided Design for Fines and Suspended-Substrate Microstrip Lines," *Int. J. Infrared Millimeter Waves*, Vol. 14, 1993, p. 1261.
8. S. Pogarsky and I. Saprykin, "Multiple Microstrip Wave Spectrum," *Int. J. Infrared Millimeter Waves*, Vol. 16, 1995, p. 209.
9. S. Ermer, D. Girton, et al., "An Electro-Optic Modulator Fabricated Using a Polyimide Doped with Thermally Stable Chromophores," *Nonlinear Opt.*, Vol. 9, 1995, p. 259.
10. B. Lyons, T. O'Ciardha, P. Herbert, and W. Kelly, "Experimental Evaluation of Coplanar Waveguide Discontinuities," *Int. J. Infrared Millimeter Waves*, Vol. 14, 1993, p. 2021.
11. B. A. Chipman, *Transmission Lines*, McGraw-Hill, New York.
12. A. Rastogi, A. Jakal, N. McEwan, and I. Khairuddin, "Loss Minimisation and Sensitivity Analysis for Coplanar Waveguides," *Int. J. Infrared Millimeter Waves*, Vol. 16, 1993, pp. 1789.
13. K. Suto, T. Kimura, and J. Nishizawa, "Tapered Waveguide Semiconductor Raman Laser," *Int. J. Infrared Millimeter Waves*, Vol. 16, 1995, p. 691.

Received 4-29-96

Microwave and Optical Technology Letters, 13/2, 90-94
 © 1996 John Wiley & Sons, Inc.
 CCC 0895-2477/96

EXPERIMENTAL EVIDENCE OF CAPACITANCE INVARIANCE OF A MULTICONDUCTOR SYSTEM UNDER LOCAL ROTATION

Xingling Zhou

Department of Electronic Engineering
 Beijing Institute of Technology
 P.O. Box 327
 Beijing, 100081, People's Republic of China

KEY TERMS

Capacitance, multiconductor system, local rotation, invariance

ABSTRACT

A new experimental discovery in electrostatics is first reported: The capacitance of a multiconductor system maintains the same value for all possible configurations, provided the geometric centers of the conductors are fixed independently. © 1996 John Wiley & Sons, Inc.

1. INTRODUCTION

As is well known, the determination of capacitance property of an arbitrary multiconductor system is important in the design and packaging of integrated circuits or other electronic systems. It is also a classical problem in electrostatics and classical field theory. In the past analytic and numerical techniques have been used to solve this problem [1]. However, calculations have been limited to simple problems such as two plates and a cube, et cetera [2, 3]. For these geometries, we can solve some cases only generally. For example, the two plates are assumed to be parallel, et cetera. It is difficult to solve exactly complicated structures, such as where two plates are not parallel. Furthermore, we have not investigated the relations among different configurations of given conductors either in theory or by experiment.

Recently, Zhou, Wang, and Zhou proposed a novel method for calculating the capacitance of an arbitrary conductor [4]. It was conjectured based on [4] and experience that the capacitance of a multiconductor system is invariant under local rotation in homogeneous medium. This means that the capacitance of a multiconductor system maintains the same value for all possible configurations, provided that the geometric centers of the conductors are fixed independently. It is verified by a simple experiment reported in this article.

2. EXPERIMENTAL WORK AND RESULTS

A WK4210 automatic LCR meter [5] shown in Figure 5 is used to measure the capacitance between two conductors. Only relative capacitance is of concern in this case; it is unnecessary to deduct possible stray capacitance completely. In spite of this, some measures, such as using shielded wires, good connections, and calibration are taken to avoid effects of stray capacitance as far as possible. Two shielded wires of diameter 2.5 mm are used to extend the two pillars. The test frequency was chosen as 10 kHz with range a between 0 and 1.6 μF and resolution of 0.001 pF. The experiment should be considered an electrostatic one, because of the low test frequency (wavelength $\lambda \approx 3 \times 10^4$ m). The auto mode was used. To avoid much higher background, the bridge must be calibrated. The constant environment condition should be kept in the experiment. The digital result representing the relative capacitance between two conductors to be measured can be read easily from its screen.